Amine-Functionalized Polyglycidyl Methacrylate Microsphere as a Unified Template for the Synthesis of Gold Nanoparticles and Single-Crystal Gold Plates

Joon Suk Oh, Luong Nguyen Dang, Sung Woon Yoon, Pyoung Chan Lee, Dong Ouk Kim, Kwang Jin Kim, Jae Do Nam*

Polyglycidyl methacrylate (PGMA) microspheres, crosslinked and surface-functionalized by amine, can be used as a solid-state template for the synthesis of gold (Au) crystals in the forms of either nanoparticles (NPs) or plates. It is discovered that the polymer microsphere acts as an internal template to cultivate Au NPs inside the microsphere or an external template to generate the single-crystal plates depending on the critical concentration (C_{cr}) of gold ions. The ion–dipole interaction and the structure-dependent solubility of gold induce two distinct gold nanostructures in the presence of the functionalized polymer microspheres. The catalytic activity and long-term storage of the developed gold nanostructures that can be easily scaled-up for mass production through the developed novel methodology is demonstrated.

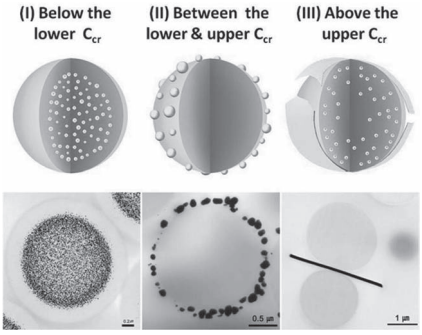

1. Introduction

Au nanostructures have been intensively studied over the past decade in various fields because of their fascinating optical, electrical, magnetic, catalytic, and biochemical properties.[1–11] Especially, numerous efforts have been devoted to controlling the shape and size of Au nanostructures, whereby their physicochemical properties are significantly changed, using various types of soft-template systems composed of surfactants or polymeric stabilizers.[12–16] For instance, anisotropic structures such as nanorods and nanoplates exhibit distinctive optical properties due to the localized surface plasmon resonance, which makes them suitable for the surface-enhanced Raman scattering technique.[10,11] Usually, colloidal self-assembies of surfactants have been employed to provide a certain structure of templates including a sphere (zero dimension), a rod (one dimension), and plate (two dimension) in the macroscopic length scale where Au nanostructures can grow into specific shapes.[17–21] In these methods, the soft templates or capping agents are frail and thus sensitive to synthesis conditions such as mechanical stirring, reaction time, temperature, and concentration.[12–15] Accordingly, difficulties are often encountered in the scaling-up production of nanomaterials.

Once the Au nanostructures are synthesized, their immobilization or separation is one of the key challenges

J. S. Oh, L. N. Dang, S. W. Yoon, P. C. Lee, J. D. Nam
Department of Polymer Science and Engineering
Sungkyunkwan University, Suwon, 440-746, South Korea
E-mail: jdnam@skku.edu
D. O. Kim
Advanced Material Research Center, Samsung Advanced Institute of Technology, Samsung Electronics., Ltd. Giheung, Yongin, 446-712, South Korea
K. J. Kim
Department of Mechanical Engineering, University of Nevada, Las Vegas, 4505 Maryland Parkway, NV 89154, USA
J. D. Nam
Department of Energy Science, Sungkyunkwan University, Suwon, 440-746, South Korea

DOI: 10.1002/marc.201200713

in practical applications, because a strong and irreversible physicochemical bonding occurs among the nanostructures and soft surfactants due to their extremely high surface energy and large surface area of nanostructures.[1,22–24] In this sense, there still remains a great need to develop a novel route that could facilitate handling and long-term storage of nanostructures in a large-volume production scale. Such a need inspired us to employ a polymer microsphere as a hard template, which is less sensitive to the reaction conditions of time, temperature, concentration, etc. as usually required in mass production. Furthermore, the hard-template system may very well allow facile separation and handling of nanostructures without raising safety issues.[25]

Herein, we report the astonishing behavior of a functionalized polymer microsphere template for the formation of Au crystals. Identifying the critical concentrations of Au precursors, we direct the microsphere as an internal template to cultivate Au NPs inside the microsphere or as an external template to guide the Au atoms to grow into Au plates in the direction along the Au {111} plane outside the microsphere. A detailed mechanism of the microsphere templating is presented and the catalytic activity and long-term storage of the developed gold nanostructures are demonstrated.

2. Experimental Section

2.1. Materials

Glycidyl methacrylate (GMA), polyvinylpyrrolidone (PVP, $\overline{M}_w \approx$ 40 000), azobisisobutyronitrile (AIBN), methanol, ethylenediamine (EDA), 4-nitrophenol (4-NP), sodium borohydride ($NaBH_4$), and hydrogen tetrachloroaurate trihydrate ($HAuCl_4$. $3H_2O$) were all purchased from Sigma-Aldrich Company and used without purification.

2.2. Preparation of Polyglycidyl Methacrylate Microspheres

The PGMA microspheres were synthesized using a dispersion polymerization method. GMA (40 g) and PVP (8 g) were dissolved in methanol (180 mL) and then the solution was purged with nitrogen for 30 min. The solution was heated to 65 °C while being stirred and an AIBN solution (pre-dissolved in 20 mL methanol) was added to the solution. The reaction was conducted at 65 °C for 12 h and the product was then washed several times with methanol and DI water using centrifugation. Finally, the PGMA microspheres were collected in powder form by freeze-drying.

2.3. Preparation of Amine-Functionalized PGMA (PGMA-ed) Microspheres

The PGMA powders (10 g) were dispersed in a mixture of ethanol and DI water (200 mL, 1/1; v/v) using mild sonication, and the suspension was then heated to 70 °C. EDA (30 mL) was added to the suspension and the reaction was conducted for 12 h. The product was then washed several times with methanol and DI water to remove the impurities using centrifugation. Finally, the product was collected through centrifugation and freeze-drying. The resulting PGMA microspheres functionalized with EDA and were labeled as PGMA-ed in this paper.

2.4. Gold Metallization with the PGMA-ed Microspheres

PGMA-ed powders (0.2 g) were dispersed in an aqueous gold solution at various concentrations of $HAuCl_4$ (5×10^{-3} M, 10×10^{-3} M, 15×10^{-3} M, and 20×10^{-3} M in 50 mL of DI water) with mild sonication. The dispersion was heated to 90 °C with gentle stirring and the reaction was conducted for 180 min. After the reaction, the products were washed with water several times and collected by centrifugation.

2.5. Catalytic Reduction of 4-Nitrophenol (4-NP) to 4-Aminophenol

Au NPs encapsulated in PGMA-ed microspheres (0.01 g, Au: 10 μmol) were dispersed in DI water (5 mL) and mixed with 4-NP (0.1 mmol, 15 mL) aqueous solution. Then, the aqueous solution of $NaBH_4$ (0.65 M, 3 mL) was added to the mixture and the reduction reaction was conducted at room temperature. The initial molar ratio of Au/4-NP/NaBH4 was 1/0.15/1950. The reaction mixture was sampled at a fixed interval through a 0.45 μm membrane filter. The rate constant of the reduction process was obtained through measuring the absorbance changes at 400 nm as a function of time.

2.6. Characterization

The morphology and elemental analysis of the sample were characterized by field emission scanning electron microscopy (FE-SEM, JEOL JSM 7000F) equipped with an energy dispersive spectrometer (EDS, EDAX Pegasus with Genesis software 6.0). An electron backscattering diffraction (EBSD, EDAX DigiView IV detector with TSL OIM analysis software 5.31) measurement was conducted on a Au plate to analyze the microstructure and the crystal orientation of it. Transmission electron microscopy (TEM) observation was carried out using a JEOL JEM 1010 at 60 kV. For the TEM observation, the samples were molded with epoxy and microtomed with a diamond knife. Au plate specimens were collected and deposited on a slide glass and analyzed using wide-angle X-ray diffraction (XRD) (Bruker AXS, D8 FOCUS) with Cu Kα radiation (λ = 0.154 nm). The XRD data were collected in the 2θ range between 30 and 90° with a scanning speed of 5° min^{-1}. The absorption spectra were recorded by UV–vis spectroscopy (Cary 5000, Varian, Inc). The polymer microspheres were characterized using Fourier transform infrared (FTIR) spectroscopy (Bruker IFS-66/S). The size distribution of samples was analyzed with Zetasizer Nano series (Malvern). An inductively coupled plasma-mass spectrometry (ICP-MS, Agilent 7500, Agilent Technologies Inc) measurement was conducted to quantify the Au ions remaining in liquid phase.

3. Results and Discussion

A uniform-sized polymer microsphere template with amine-functional groups was fabricated by using dispersion polymerization of glycidyl methacryalte and subsequent amine-functionalization with EDA. Figure S1 (Supporting Information) represents the chemical structures of the PGMA and amine-modified PGMA (PGMA-ed) microspheres (before and after the functionalization process, respectively) and compares their FT-IR spectra, demonstrating that most of the epoxy groups in the PGMA microspheres react with EDA to give amine-functionalized microspheres. The amine groups in PGMA-ed allows the Au ions to be immobilized in the microsphere by the ion–dipole attractive interaction between the electron pairs of amine and Au atoms.[26] Then, the immobilized Au ions in the PGMA-ed microspheres can be metallized in-situ by the thermal reduction process.

Figure 1 presents the SEM (a to d) and cross-sectional TEM (e to h) images of samples after the metallization process at varied concentrations (5×10^{-3} M, 10×10^{-3} M, 15×10^{-3} M, and 20×10^{-3} M) of Au sources. At a 5×10^{-3} M concentration, we found that Au NPs were formed mostly inside the PGMA-ed. The SEM image (Figure 1a) shows the smooth surface of the microspheres with no Au NPs, while the cross-section TEM image (Figure 1e) shows Au NPs with a diameter ranging from 3 to 20 nm distributed densely inside the PGMA-ed (the inset shows the magnified TEM image). It suggests that the majority of the Au ions are absorbed inside the PGMA-ed microsphere and thermally reduced in situ, which consequently provides the encapsulated Au NPs. When the metal ions are reduced while entrapped in the hydrated polymer network, the nucleated metallic seeds tend to grow larger and produce well-dispersed NPs with sizes of 5–20 nm. This growth is caused by the collection of the metal ions around the nuclei until all the ions in the hydrated polymer are consumed.[27] Since the metallization of Au ions occurs when they are immobilized within the microspheres, the amount of Au loading can be readily controlled by varying the Au concentrations ($0.3–3 \times 10^{-3}$ M). Figure S2 (Supporting Information) displays the cross-sectional TEM images in regards to various loading densities of encapsulated Au NPs and the digital image of their suspension, which confirms the gradual increases in the Au NPs loading.

In contrast, at a 10×10^{-3} M concentration, Au NPs were formed mostly on the surface of the PGMA-ed, which can be found in SEM and TEM images (Figure 1b and f). At this condition, it appears that the nucleation of Au ions begins to occur on the surface of PGMA-ed rather than inside, then the nucleated seeds on the surface grow larger by consuming the Au ions around them. We presume that the nucleation sites are shifted from inside to the surface region when the concentration of Au sources exceeds the saturated concentration at which the PGMA-ed is fully occupied with Au ions. It is strongly estimated that the activity of the PGMA-ed surface is higher than that of inside because the functionalization degree in the surface is somewhat higher than that inside the microsphere. It was confirmed through EDS analysis of a microtomed PGMA-ed microsphere, which showed the vicinity of the microsphere edge had slightly higher nitrogen content than the center (Figure S3, Supporting Information). The saturated concentration appears to be between

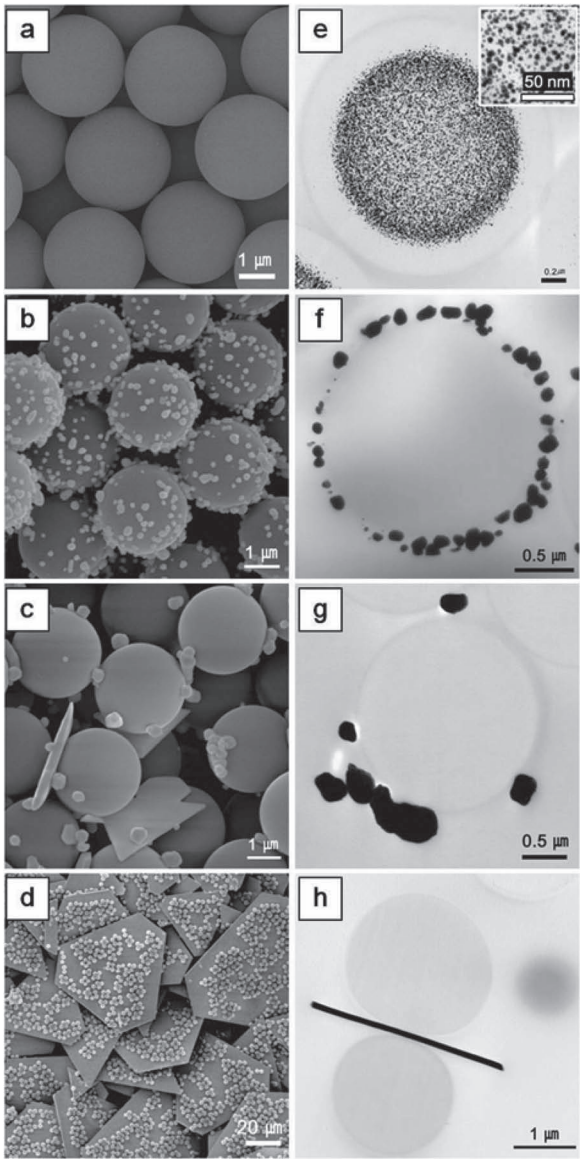

Figure 1. SEM (a to d) and cross-sectional TEM (e to h) images showing Au NPs and single-crystal Au plates produced inside or on the surface of the PGMA-ed microspheres. Thermal metallization was taken at various concentrations of $HAuCl_4$; a and e at 5×10^{-3} M, b and f at 10×10^{-3} M, c and g at 15×10^{-3} M, and d and h at 20×10^{-3} M.

5×10^{-3} and 10×10^{-3} M of $HAuCl_4$, which we define as the lower C_{cr} herein that regulates the nucleation position in the PGMA-ed.

When the concentration of Au sources increases to 15×10^{-3} M, the Au NPs grow up to hundreds of nanometers larger and a small portion of plate structures of Au in several micrometers are detected together (Figure 1c,g). When the concentration reaches 20×10^{-3} M, a noticeable structural transformation of Au crystals takes place. The SEM image (Figure 1d) shows a large number of Au plates (tens of micrometers in width) with PGMA-ed attached on their basal planes. The TEM image (Figure 1h) shows the cross-section of a Au plate with the thickness around 90 nm located between microspheres. The Au plates and the microspheres can be easily separated thorough mild sonication. Figure S4 (Supporting Information) illustrates SEM images of the separated Au plates that are mostly composed of triangular, truncated triangular, and hexagonal shapes. Most of the observed plates had sharp edges and clear, flat surfaces with no grain boundaries suggesting that a single-crystalline structure was grown preferentially in the direction along the Au {111} plane (see more detailed explanation and data in Supporting Information).

It has been reported that the rapid (thermodynamically controlled) reduction of metal ions produces spherical NPs, but that their slow (kinetically controlled) reduction produces plate structures.[28] In our experiments, the reduction took less than 15 min when the concentration was below 15×10^{-3} M and more than 120 min above 20×10^{-3} M to achieve a conversion degree higher than 99.9%. Considering the reduction times and the structural transformation of Au crystals, a thermodynamically controlled reduction occurs below the 15×10^{-3} M of Au sources while a kinetically controlled reduction arises above the 20×10^{-3} M in our experimental conditions. It indicates that there is a certain concentration, designated as the upper C_{cr}, between 15×10^{-3} M and 20×10^{-3} M of Au sources that directs the growth rate of Au crystals, which eventually changes the structures of Au from nanospheres into plates.

A more detailed examination was conducted to identify the growth of the Au plates in reaction time. Figure 2a–f displays the cross-sectional TEM images of PGMA-ed microspheres collected at 0, 30, 60, 90, 120, and 180 min of reaction at a 20×10^{-3} M of $HAuCl_4$. The interior of PGMA-ed is dark in the early stage of the reaction due to the absorbed Au ions inside. As the reaction proceeds, it gradually turns light indicating that the Au ions diffuse out of the PGMA-ed (Figure 2a–f). Meanwhile, those Au ions accumulated on the microsphere surface are converted to a thin Au shell with a thickness of around 25 nm

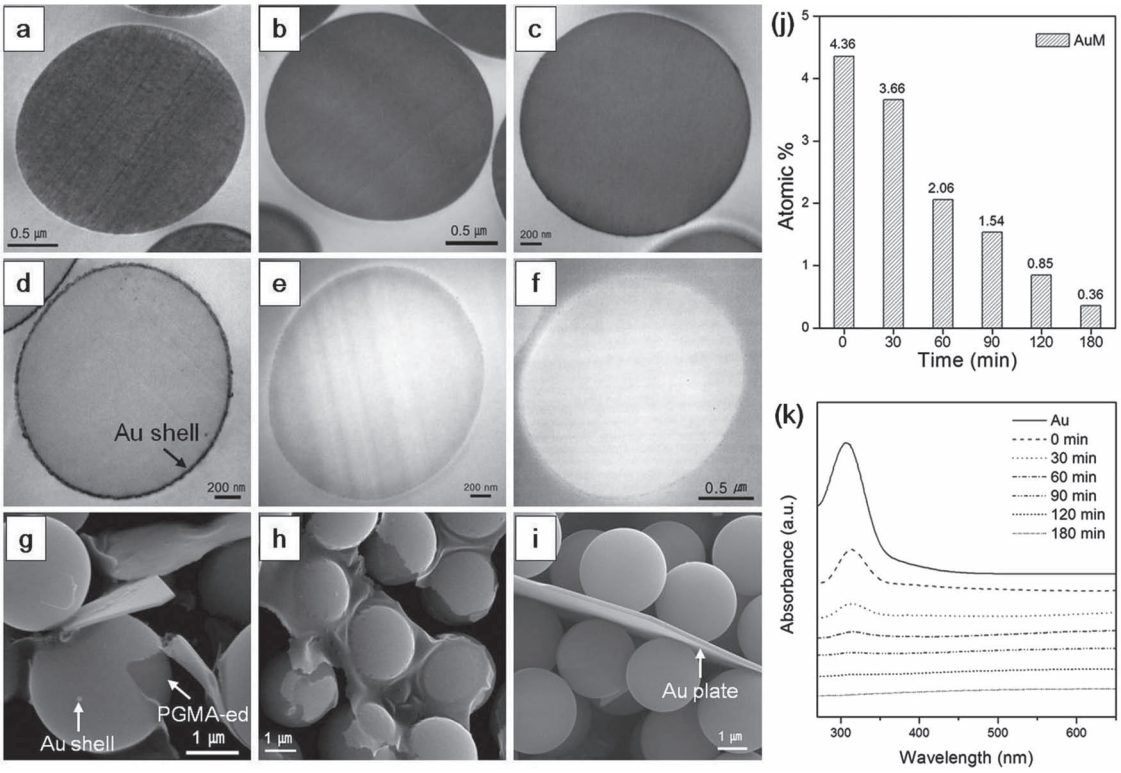

Figure 2. Cross-sectional TEM images of PGMA-ed microspheres at a 20×10^{-3} M of $HAuCl_4$ after different thermal reduction time of (a) 0, (b) 30, (c) 60, (d) 90, (e) 120, and (f) 180 min and SEM images of the samples from the reduction time of (g) 90, (h) 120, and (i) 180 min. Au atomic percentages of the samples above were obtained by EDS (j) and the UV–Vis absorption spectra (i) of liquid media were each collected at different reaction times. In the UV–Vis spectra, Au represents $HAuCl_4$ solution w/o microspheres.

(Figure 2d). The Au shell is seemingly detached from the microsphere surface during the continuous reaction under mechanical agitation (Figure 2e,f), which is further confirmed through SEM observation (Figure 2g,h) exhibiting a thin Au shell and its fragments detached from the PGMA-ed surface. The shell and fragments appear to gradually grow into the Au plates up to tens of micrometers preferentially in the direction along the Au {111} plane (Figure 2i). Although not found in the TEM images, Au NPs might be formed inside and in the vicinity of the microsphere surface in the early stage of synthesis, but the Au atoms are likely to migrate to form a kinetically favorable structure complying with the Gibbs-Thomson relation, where the relative solubility of a curved solid surface (S_c), e.g., a sphere with a radius (R), to the a flat surface ($S\infty$) can be expressed as below[29]

$$\ln\left(\frac{S_c}{S_\infty}\right) = \frac{2\gamma\Omega}{kRT} \quad (1)$$

where γ is the surface tension, Ω is the atomic volume, k is the Boltzmann constant, and T is temperature. When two different curvatures, a Au nanosphere and a Au nanoplate, are present together, the solubility of the former is relatively much higher than that of the latter, which leads to the dissolution of the Au nanosphere and growth of the Au nanoplate.

As seen in Figure 2j, the atomic percentage of Au inside the PGMA-ed constantly decreases as the reaction proceeds (detailed EDS spectra is in Figure S5, Supporting Information), which also confirms that the Au ions are gradually diffused out of the PGMA-ed. Figure 2k presents the UV–vis spectra of the liquid media at the corresponding reaction time. The peak around 320 nm, assigned to $AuCl_4^-$,[30] abruptly decreases immediately after the addition of PGMA-ed into the $HAuCl_4$ solution due to the absorption of Au ions by PGMA-ed. The peak intensity continuously weakens and finally disappears after 90 min of reaction. The results indicate that the Au ions residing inside and outside the PGMA-ed are converted into Au plates simultaneously and continuously.

Based on the findings, the mechanism schematically represented in Figure 3 is proposed. As seen in Figure 3a, when the Au ions are added to the PGMA-ed below the lower C_{cr}, the majority of the Au ions are absorbed inside the microspheres due to the ion–dipole interaction between the amine groups and Au atoms. Upon heating, the nucleation of the Au ions begins to occur inside the polymer network of microspheres; subsequently, the Au ions migrate to the nuclei and grow larger until the Au ions around the nucleated sites are consumed. Under this condition, the PGMA-ed microsphere acts as an internal template cultivating Au NPs inside the microsphere.

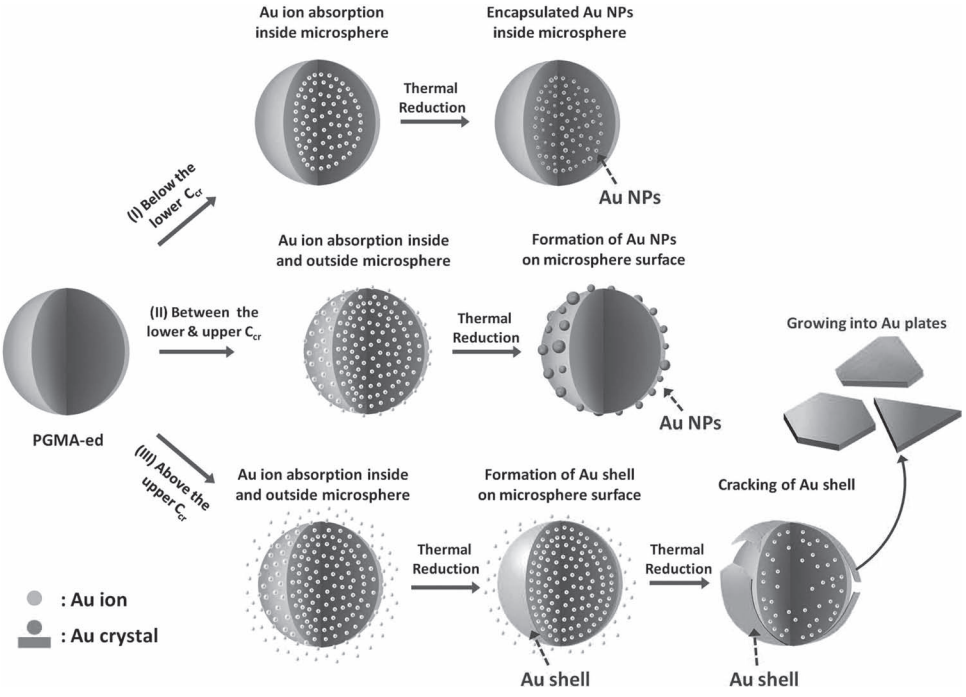

Figure 3. Schematic illustration showing the formation of Au crystals with different structures generated either inside or outside the PGMA-ed microspheres by adjusting the concentration of Au sources. Au NPs are formed inside the microsphere below the lower C_{cr} (I), formed on the surface between the lower and upper C_{cr} (II), and single-crystal Au plates are grown on the surface above the upper C_{cr} (III).

As the concentration exceeds the lower C_{cr}, the templating nature of the PGMA-ed alters its function as an external template to produce Au NPs on its surface (Figure 3b). It is assumed that the nucleation of Au ions initiates on the surface of the PGMA-ed when it is fully saturated with Au ions. Once Au nuclei are formed on its surface, they continuously grow by consuming the Au ions around them, which gives Au NPs with diameters from tens to hundreds of nanometers supported on the PGMA-ed surface.

A different reaction mechanism took place above the upper C_{cr} of $HAuCl_4$. Figure 3c displays the growth of Au plates in the presence of the PGMA-ed. As with various soft template systems used for the synthesis of metal nanocrystals, the primary metal particles are formed at a very early stage of the reaction in the presence of templates and the particles are self-assembled within the templates followed by sintering in a certain direction to become larger crystals.[17–21] Accordingly, we presume that the outer surface of the PGMA-ed microsphere may act as a monolayer template, where a thin Au shell is formed in the early stage of the reaction and subsequently peeled off from the surface under mechanical agitation. Afterwards, the shell and its fractures grow into a single-crystal Au plate preferentially in the {111} lattice plane. As well as the templating effect, a kinetically controlled growth of Au crystals begins to occur above the upper C_{cr}, which favorably controls the Au structures to grow into plate structures.

Catalytic activity of the Au NPs encapsulated within the PGMA-ed (Au/PGMA-ed) was investigated by the reaction of 4-nitrophenol (4-NP) to 4-aminophenol (4-AP) in the presence of $NaBH_4$ as a reductant.[31] The progress of the reduction reaction was observed by UV–vis spectroscopy (Figure 4a). As can be seen, the characteristic peak of 4-NP at 400 nm decreases over time and completely disappears after 20 min while a peak of 4-AP at 290 nm gradually increases. Even though the Au NPs are entrapped in the polymer matrix, they exhibits catalytic activity. It is expected that the hydrophilic nature of the PGMA-ed allows 4-NP to diffuse inside the Au/PGMA-ed microspheres and contact Au NPs for the production of 4-AP. Regarding it as a pseudo-first-order reaction,[32] the rate constant (k) can be calculated from a linear relation of $\ln(A_0/A_t)$ with time (t), where A_t is absorbance (400 nm) at time t, and A_0 is absorbance at the initial stage. Figure 4b shows the linear plot of $\ln(A_0/A_t)$ versus the reaction time at room temperature, giving the rate constant from the slope as 3.8×10^{-3} s^{-1}, which is comparable with other Au NP catalytic systems.[33,34] After the catalytic reaction, the Au/PGMA-ed microspheres were completely separated from the solution by a simple filtration method. Furthermore, undesired aggregations of NPs, arising during catalytic reactions, can be effectively avoided because

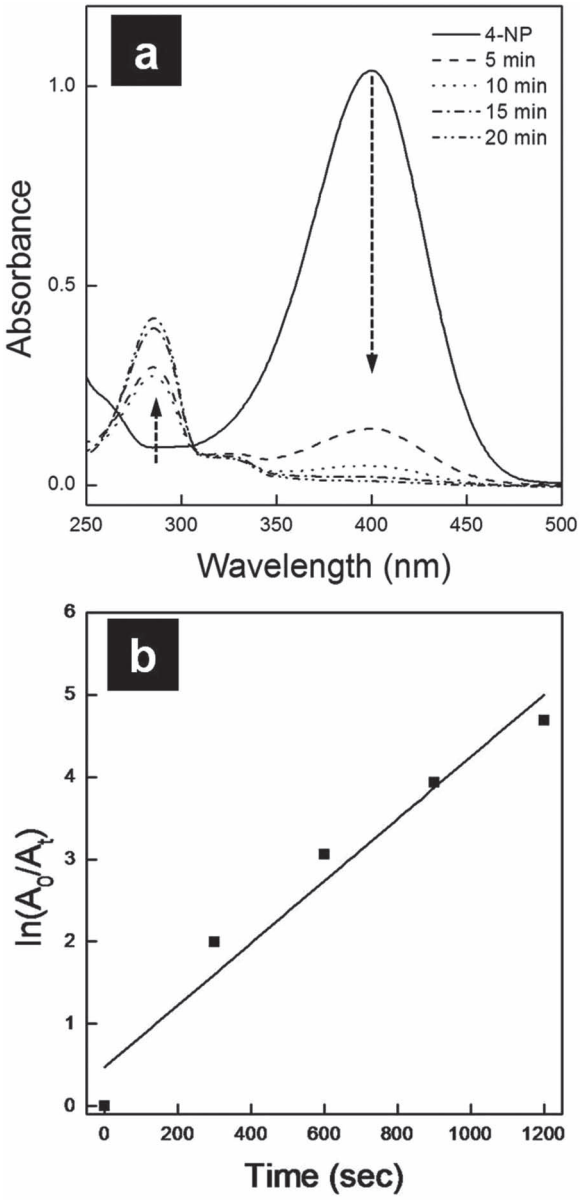

Figure 4. UV–vis absorption spectra for the catalytic reduction of 4-nitrophenol to 4-aminophenol in aqueous media at room temperature (a). Plot of $\ln(A_o/A_t)$ versus time for the reduction of 4-NP (b).

they are physically isolated in a confined space within the polymer matrix.

It is important to note that the developed Au/PGMA-ed microspheres are mechanically hard and can be obtained as a fine powder form through a drying process. This option allows long-term storage of Au NPs in the daily environment. The Au/PGMA-ed powders kept for several months can be easily re-dispered in solvents without aggregations, which is confirmed by the particle size distribution measurement. The distribution of Au/PGMA-ed microspheres dispersed in water is almost similar with

that of PGMA-ed, demonstrating the high dispersibility of Au/PGMA-ed (Figure S6, Supporting Information). In addition, the production quantity of the Au/PGMA-ed can be readily scaled-up to several tens of grams with a controlled loading density in the laboratory. For example in our case, we were able to obtain 12.2 g of them in a single batch in the forms of solution or powder (Figure S7, Supporting Information). It is believed that these features, as well as long-term storage and large-scale production, are highly desirable for practical applications in various fields.

4. Conclusions

Two distinct structures of Au crystals were produced in the presence of the PGMA-ed microsphere as either an internal or external template depending on the concentration of Au sources. We discovered that both the lower and upper C_{cr} of Au sources were the main key factors to ensure the production of different structures. Below the lower C_{cr}, the polymer microsphere acted as a microreactor for the incubation of the Au NPs, in which the loading density of the Au NPs can be readily controlled by the quantity of the Au sources. Above the lower C_{cr}, the microsphere shifted to an external template to form Au NPs mostly on its surface. As the concentration exceeded the upper C_{cr}, a large quantity of single-crystalline Au plates were formed with the aid of the PGMA-ed, where the PGMA-ed and Au plates were easily separated through mild sonication. The Au/PGMA-ed microspheres were able to be dried into a powder form enabling long-term storage and exhibited catalytic activity in converting 4-NP to 4-AP with the rate constant of 3.8×10^{-3} s^{-1}.

Solid state polymer beads with controlled size and functionality are highly anticipated as unified reactive templates for the synthesis of various types and structures of metal NPs which would be very useful in a wide spectrum of future catalytic and optoelectronic applications.

Supporting Information

Supporting Information is available from the Wiley Online Library or from the author.

Acknowledgements: This research was supported by the WCU (World Class University) program through the Korea Science and Engineering Foundation funded by the Ministry of Education, Science and Technology (R31-2008-000-10029-0). We also appreciate the project and equipment support from Gyeonggi Province through the GRRC program in Sungkyunkwan University. K.J.K. appreciate the partial financial support from the U.S. Office of Naval Research (N000140910218).

Received: November 5, 2012; Revised: December 21, 2012; Published online: January 25, 2013; DOI: 10.1002/marc.201200713

Keywords: catalysts; gold nanocrystals; gold nanoparticles; polymer microspheres;

[1] M. C. Daniel, D. Astruc, *Chem. Rev.* **2004**, *104*, 293.
[2] Y. Sun, Y. Xia, *Science* **2002**, *298*, 2176.
[3] S. Eustis, M. A. El-Sayed, *Chem. Soc. Rev.* **2006**, *35*, 209.
[4] R. Elghanian, J. J. Storhoff, R. C. Mucic, R. L. Letsinger, C. A. Mirkin, *Science* **1997**, *277*, 1078.
[5] J. N. Anker, W. P. Hall, O. Lyandres, N. C. Shah, J. Zhao, R. P. Van Duyne, *Nat. Mater.* **2008**, *7*, 442.
[6] Q. Zhang, J. Xie, J. Yang, J. Y. Lee, *ACS Nano* **2008**, *3*, 139.
[7] M. Haruta, M. Daté, *Appl. Catal., A* **2001**, *222*, 427.
[8] M. Valden, X. Lai, D. W. Goodman, *Science* **1998**, *281*, 1674.
[9] W. Lu, S. R. Arumugam, D. Senapati, A. K. Singh, T. Arbneshi, S. A. Khan, H. Yu, P. C. Ray, *ACS Nano* **2010**, *4*, 1739.
[10] W. H. Yang, G. C. Schatz, R. P. Van Duyne, *J. Chem. Phys.* **1995**, *103*, 869.
[11] B. J. Wiley, D. J. Lipomi, J. Bao, F. Capasso, G. M. Whitesides, *Nano Lett.* **2008**, *8*, 3023.
[12] X. Sun, S. Dong, E. Wang, *Angew. Chem. Int. Ed.* **2004**, *43*, 6360.
[13] W. L. Huang, C. H. Chen, M. H. Huang, *J. Phys. Chem. C* **2007**, *111*, 2533.
[14] C. Kan, X. Zhu, G. Wang, *J. Phys. Chem. B.* **2006**, *110*, 4651.
[15] B. Liu, J. Xie, J. Y. Lee, Y. P. Ting, C. J. Paul, *J. Phys. Chem. B.* **2005**, *109*, 15256.
[16] Y. Shao, Y. Jin, S. Dong, *Chem. Commun.* **2004**, *10*, 1104.
[17] M. P. Pileni, *Nat. Mater.* **2003**, *2*, 145.
[18] T. K. Sau, A. L. Rogach, *Adv. Mater.* **2010**, *22*, 1781.
[19] S. S. Shankar, A. Rai, B. Ankamwar, A. Singh, A. Ahmad, M. Sastry, *Nat. Mater.* **2004**, *3*, 482.
[20] B. A. Simmons, S. Li, V. T. John, G. L. McPherson, A. Bose, W. Zhou, J. He, *Nano Lett.* **2002**, *2*, 263.
[21] A. K. Boal, F. Ilhan, J. E. Derouchey, T. Thurn-Albrecht, T. P. Russell, V. M. Rotello, *Nature* **2000**, *404*, 746.
[22] A. Biffis, S. Cunial, P. Spontoni, L. Prati, *J. Catal.* **2007**, *251*, 1.
[23] T. F. Jaramillo, S. H. Baeck, B. R. Cuenya, E. W. McFarland, *J. Am. Chem. Soc.* **2003**, *125*, 7148.
[24] X. Shi, S. Wang, S. Meshinchi, M. E. Van Antwerp, X. Bi, I. Lee, J. R. Baker Jr, *Small* **2007**, *3*, 1245.
[25] D. B. Warheit, C. M. Sayes, K. L. Reed, K. A. Swain, *Pharmacol. Ther.* **2008**, *120*, 35.
[26] K. K. Chia, R. E. Cohen, M. F. Rubner, *Chem. Mater.* **2008**, *20*, 6756.
[27] P. C. Lee, T. H. Han, D. O. Kim, J. H. Lee, S. J. Kang, C. H. Chung, Y. Lee, S. M. Cho, H. G. Choi, T. Kim, E. Lee, J. D. Nam, *J. Membr. Sci.* **2008**, *322*, 441.
[28] Y. Xiong, J. M. McLellan, J. Chen, Y. Yin, Z. Y. Li, Y. Xia, *J. Am. Chem. Soc.* **2005**, *127*, 17118.
[29] R. Vook, *Inter. Met. Rev.* **1982**, *27*, 209.
[30] K. Esumi, A. Suzuki, N. Aihara, K. Usui, K. Torigoe, *Langmuir* **1998**, *14*, 3157.
[31] Y. Mei, G. Sharma, Y. Lu, M. Ballauff, M. Drechsler, T. Irrgang, R. Kempe, *Langmuir* **2005**, *21*, 12229.
[32] Y. Wang, G. Wei, W. Zhang, X. Jiang, P. Zheng, L. Shi, A. Dong, *J. Mol. Catal. A: Chem.* **2007**, *266*, 233.
[33] M. Zhang, L. Liu, C. Wu, G. Fu, H. Zhao, B. He, *Polymers* **2007**, *48*, 1989.
[34] H. Wu, Z. Liu, X. Wang, B. Zhao, J. Zhang, C. Li, *J. Colloid Interface Sci.* **2006**, *302*, 142.